The Lifetime of Inositol 1,4,5-trisphosphate in Single Cells

SAMUEL S.-H. WANG,* ADAWIA A. ALOUSI, and STUART H. THOMPSON*

From the *Neurosciences Program and Hopkins Marine Station of Stanford University, Pacific Grove, California 93950

ABSTRACT In many eukaryotic cell types, receptor activation leads to the formation of inositol 1,4,5-trisphosphate (IP_3) which causes calcium ions (Ca) to be released from internal stores. Ca release was observed in response to the muscarinic agonist carbachol by fura-2 imaging of N1E-115 neuroblastoma cells. Ca release followed receptor activation after a latency of 0.4 to 20 s. Latency was not caused by Ca feedback on IP_3 receptors, but rather by IP_3 accumulation to a threshold for release. The dependence of latency on carbachol dose was fitted to a model in which IP_3 synthesis and degradation compete, resulting in gradual accumulation to a threshold level at which Ca release becomes regenerative. This analysis gave degradation rate constants of IP_3 in single cells ranging from 0 to 0.284 s^{-1} (0.058 ± 0.067 s^{-1} SD, 53 cells) and a mean IP_3 lifetime of 9.2 ± 2.2 s. IP_3 degradation was also measured directly with biochemical methods. This gave a half life of 9 ± 2 s. The rate of IP_3 degradation sets the time frame over which IP_3 accumulations are integrated as input signals. IP_3 levels are also filtered over time, and on average, large-amplitude oscillations in IP_3 in these cells cannot occur with period < 10 s.

INTRODUCTION

Inositol 1,4,5-trisphosphate (IP_3) plays a central role in mobilizing calcium in eukaryotic cells (Berridge and Irvine, 1989; Rana and Hokin, 1990). The activation of neurotransmitter or hormone receptors on the cell surface causes G-protein–mediated activation of phosphoinositide-specific phospholipase C (PLC). PLC converts phosphatidyl-1,4-bisphosphate (PIP_2) in the plasma membrane to IP_3 and diacylglycerol (Rhee, Suh, Ryu, and Lee, 1989) and IP_3 activates channels in the endoplasmic reticulum to cause the release of stored calcium ions (Ca) into the cytoplasm. IP_3-dependent Ca release can occur in a spatially and temporally organized manner, taking the form of oscillations or waves which cross within and between cells (Berridge, 1990; Jaffe, 1991).

The lifetime of IP_3 determines whether regenerative IP_3 production could underlie the propagation of a Ca wave. Ca waves cross cells without diminishing or slowing

Address correspondence to Dr. Wang at his current address, Department of Neurobiology, P.O. Box 3209, Duke University Medical Center, Durham, NC, 27710.

J. GEN. PHYSIOL. © The Rockefeller University Press · 0022-1295/95/01/0149/23 $2.00
Volume 105 January 1995 149–171

and are, therefore, generated by a process in which a messenger is regeneratively produced (Winfree, 1987). In one possible mechanism, the diffusion of locally produced IP_3 is rate limiting (Allbritton, Meyer, and Stryer, 1992), and a wave of IP_3 accompanies the Ca wave as it crosses the cell. No indicator is available that would allow IP_3 to be visualized. However, knowledge of the lifetime of IP_3 is useful in calculating whether a concentration gradient of IP_3 might exist at the time of wave initiation.

The lifetime and diffusion constant of IP_3 in cytoplasm also together determine its spatial range of action. These variables have been measured under certain conditions (Allbritton et al., 1992; Irvine, Änggård, Letcher, and Downes, 1985; Stauderman, Harris and Lovenberg, 1988; Breer, Boekhoff, and Tarelius, 1990), but little is known about how quickly IP_3 is degraded in single cells. The rate of second messenger degradation is of particular interest in spatially extended structures such as dendritic arbors. Computational models of the spread of second messengers from a dendritic spine to neighboring spines predict that biochemical signals are compartmentalized and that the rate of messenger removal is critical in this function (Koch and Zador, 1993).

In this study, the delay to calcium release was used to infer the lifetime of IP_3 in individual cells. This analysis was predicated on the steep dose-response curve of IP_3 action upon its receptor (Meyer, Holowka, and Stryer, 1988; Parker and Ivorra, 1992). This was used in a simple model of IP_3 accumulation and degradation, in which Ca release begins when IP_3 levels reach a threshold. The dose dependence of latency could then be used to derive the rate of IP_3 degradation in single cells. For comparison, the lifetime of IP_3 was determined independently by direct biochemical assay. Results from the two measures agreed with one another.

Our preparation for the study of IP_3-mediated Ca release is the mouse neuroblastoma cell line N1E-115, which expresses muscarinic M1 acetylcholine receptors (McKinney and Richelson, 1984, 1986; Mathes, Wang, Vargas, and Thompson, 1992). N1E-115 cells are well suited for the work described here. Like many eukaryotic cells, they have the IP_3 production and Ca release machinery (Surichamorn, Forray, and El-Fakahany, 1990). The low expression of muscarinic receptors (Fisher and Snider, 1987) allows the kinetics of Ca release to act as a sensitive assay for receptor activation. Finally, these cells do not form cholinergic synapses (Kimura, Oda, Deguchi, and Higashida, 1992) so that evoked responses are the direct result of receptor activation.

MATERIALS AND METHODS

Cell Culture

N1E-115 neuroblastoma cells were obtained from the UCSF Cell Culture Facility, maintained without antibiotics in Dulbecco's Modified Eagle Medium (Sigma Chemical Co., St. Louis, MO) and 10% fetal bovine serum (Hyclone), and subcultured once a week. For experiments, cells were plated on cover slips and grown to 60–80% confluence; at this time the medium was replaced with differentiation medium containing 2% dimethylsulfoxide (Kimhi, Palfrey, Spector, Barak, and Littauer, 1977). Cells were used 7–21 d after differentiation.

Calcium Imaging

Cells were loaded with the calcium indicator fura-2 by bathing in a solution containing 5 μM fura-2/AM (Molecular Probes, Inc., Eugene, OR) and 0.025% pluronic acid F-127 (Molecular Probes, Inc.) for 60 min at 20°C. After loading, the cells were rinsed and transferred to an experimental chamber. Loading with other, additional chelators was achieved by incubating cells with AM ester while they were on the microscope stage. The resulting second buffer load was estimated to be 25–100 μM by measuring the attenuation of $[Ca]_i$ rises in response to high-potassium depolarization (Wang, S. S.-H., and S. H. Thompson, manuscript in preparation). Fluorescence imaging was performed on a Nikon Diaphot epifluorescence microscope equipped with 20× Fluor objective (Nikon), Hamamatsu C2400 silicon-intensified target camera and a Sony VHS video tape recorder. Excitation illumination by a Xenon arclamp was filtered through 10-nm bandpass interference filters centered at 340 and 380 nm (Corion Corp., Holliston, MA), which were mounted on a computer-controlled filter wheel. Calibration of fluorescence to units of calcium was performed off line using a pipeline image processor (MegaVision, Santa Barbara, CA). Background-subtracted and frame-averaged F_{340}/F_{380} ratios were calibrated using standard solutions of fura-2 between two cover slips according to the equations of Grynkiewicz, Poenie, and Tsien (1985). The measured calibration parameters were $R_{min} = 0.072 \pm 0.004$, $R_{max} = 2.44 \pm 0.04$, (F_{min}/F_{max}) at 380 nm = 21.0 ± 0.8.

Ca kinetics were resolved by monitoring the cells continuously for up to 60 s at 380 nm excitation after first obtaining F_{340}/F_{380}. Because dye fade during this period was insignificant, only an initial ratiometric determination was needed at the beginning of each record. The initial F_{380} and $[Ca]_i$ in a single cell then allowed the calculation of F_{min} and F_{max}, F_{380} values corresponding to zero and saturating Ca concentrations, using the following equations:

$$F_{max} = F_{380} \cdot (1 + [Ca]_i/K_D)/(\sigma + [Ca]_i/K_D)$$

$$F_{min} = \sigma \cdot F_{max},$$

where $\sigma = F_{380,min}/F_{380,max}$ and is a constant of the imaging system. $[Ca]_i$ at later times could then be calculated from F_{380} using the Henderson-Hasselbalch equation, as is done for single-wavelength dyes (Kao, Harootunian, and Tsien, 1989). A similar procedure has been employed by other investigators (Neher and Augustine, 1992). From resting $[Ca]_i$ levels between 30 and 110 nM (68 ± 39 nM, 182 cells), a 25% change in F_{380} corresponds to a change in $[Ca]_i$ of 126 ± 15 nM.

Drug Applications

Carbachol solutions were applied by total, vigorous replacement of the chamber saline using a computer-controlled perfusion device. Six successive exchanges with normal saline at the end of the drug application ensured that no drug remained in the chamber. The external saline contained (in millimolar): NaCl, 137; KCl, 5.4; $CaCl_2$, 1.8; $MgSO_4$, 0.8; KH_2PO_4, 0.4; Na_2HPO_4, 0.3; glucose, 23; and NaHEPES, 20 (pH 7.4, T = 27–30°C). A 15–30 min recovery period between agonist applications ensured the reproducibility of the response.

IP_3 Determinations

IP_3 determinations were done by competitive radioligand binding displacement of $[^3H]$-IP_3 from a binding protein obtained from bovine adrenal granules (Palmer, Hughes, Lee, and Wakelam, 1989; No. TRK, 1000, Amersham Life Sciences, Arlington Heights, IL). On the day of the experiment, the medium was decanted, the cells were washed with 2 × 2 ml normal external saline (pH 7.4 at 30°C), and vehicle or 1 mM carbachol was added for 30 s. The reaction was either stopped immediately or continued in the presence of 10 μM atropine for

10–30 s. At the end of the drug exposure, the cover slip was transferred to another petri dish and the reaction was stopped with ice-cold 20% perchloric acid. The acid cell lysate was transferred to a microfuge tube and the precipitated protein was separated by centrifugation. The assays were done as specified in the kit. The pH of the PCA lysate was adjusted to 7.5 using 10 μl 1 N KOH in the presence of 2 μl Universal Indicator (Eastman Kodak Co., Rochester, NY) and the precipitated potassium perchlorate was removed by centrifugation. 100 μl of the supernatant was used to displace binding in ice-cold microfuge tubes containing 100 μl buffer (0.1 M Tris, 4 mM EDTA, 4 mg/ml BSA, pH 9.0); 100 μl (~2.5 kilobecquerels activity) (D-myo-[^{3}H]-IP_3); and 100 μl IP_3-specific binding protein. After vortex mixing and incubation on ice for 15 min, the tubes were centrifuged and the bottom part of the tube containing the protein was cut with a razor and transferred to a vial for scintillation counting. A standard curve for IP_3 ranging from 0.19 to 25 pmol IP_3 was prepared simultaneously in the same way as the unknown.

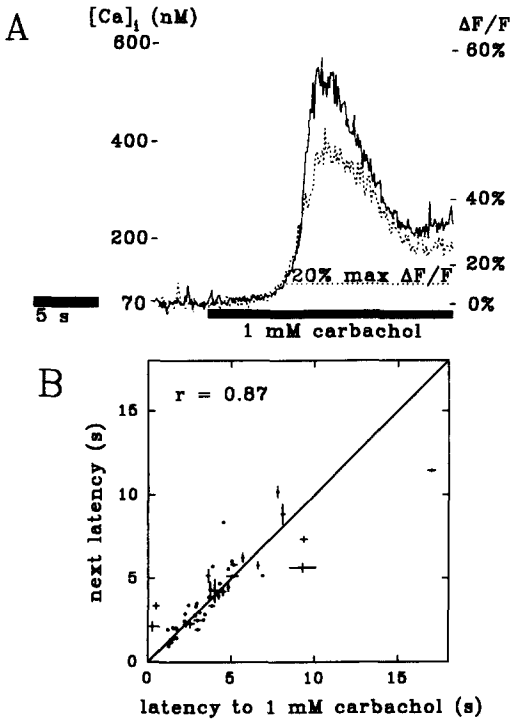

FIGURE 1. Calcium mobilization in N1E-115 cells evoked by carbachol. (*A*) Recordings made at 380 nm excitation from a cell loaded with fura-2/AM. Exposure to 1 mM carbachol at 27°C led to release of Ca from internal stores. After 30 s, the agonist was washed out, and after a 15-min rest, a second application of 1 mM carbachol was made (*dotted trace*). Latency was defined as the time taken to reach 20% of the peak change in fluorescence (see Materials and Methods). Rise time was defined as the time taken from 20 to 80%. (*B*) Latency to two consecutive doses of 1 mM carbachol. The latency is a reproducible parameter in individual cells (r = 0.87, 59 cells).

Latency and Rise Time Analysis

Rises in $[Ca]_i$ in response to carbachol application were preceded by a period during which little or no change in $[Ca]_i$ could be seen (Fig. 1 *A*). This period, latency, was defined as the time between initial presentation of agonist and the time of fluorescence change 20% of the way to peak $[Ca]_i$. Rise time was defined as the time from 20% to 80% fluorescence change. These times were calculated by fitting traces of F_{380} fluorescence sampled 3–30 times/s. Baseline F_0 and peak ΔF were calculated from the trace. The time at which the fluorescence trace crossed the criterion point (20% or 80% change from baseline toward peak) was calculated by fitting the data for 2–4 samples on either side of the crossing point to a linear function. Uncertainty in the

crossing time was calculated from the estimated error of the fit (Bevington, 1969). Fits were accepted if (*a*) peak $\Delta F/F_0 > 0.1$. (*b*) The peak ΔF was attained more than four samples before the end of the recording period (usually 30 s). (*c*) Uncertainty in the time was less than two sample intervals. All data were corrected to take into account the dead time of the drug application system, ~0.5 s. Dead time was measured by exchanging a clear solution for one containing methylene blue, and vice versa.

RESULTS

The muscarinic agonist carbachol mobilizes calcium in differentiated N1E-115 neuroblastoma cells. Responses from a cell exposed to 1 mM carbachol are shown in Fig. 1 *A*. The initial phase of Ca release is characterized by a period during which little or no change in $[Ca]_i$ is observed. We defined latency as the length of the interval from the beginning of agonist exposure to the time at which F_{380} fura-2 fluorescence had decreased 20% of the way to its first minimum. Latency varied between 0.4 and 20 s (average for 1 mM carbachol 5.8 ± 3.9 (SD) s, 130 cells in four experiments). After allowing a recovery period of at least 15 min for the Ca stores to be restored to their initial state, subsequent applications of the same concentration of carbachol resulted in approximately equal latencies (Fig. 1 *B*; $r = 0.87$, $n = 59$ cells). The latency to a given dose of carbachol was unchanged even after up to five 30-s agonist challenges. Another reproducible quantity was rise time, defined as the time needed for F_{380} to change from 20 to 80% of its total peak value (average rise time 2.8 ± 2.1 s, $r = 0.87$, 53 cells). Some cells showed oscillations in Ca for as long as agonist was present; these too were reproducible. In some cases, the peak $[Ca]_i$ decreased with successive applications of carbachol, possibly reflecting the filling state of the stores or a redistribution of dye.

Could latency result from the buildup of IP_3? If this were so, then pretreatment with a low dose of agonist would shorten the latency to a second, higher dose of agonist by stimulating the formation of a subthreshold amount of IP_3. Fig. 2 *A* shows two recordings from a cell exposed to 1 mM carbachol. For the second (*dashed*) trace the application of 1 mM carbachol was preceded by a prepulse of 100 μM carbachol lasting 10 s. This shortened the latency from 6.6 to 3.6 s. During the prepulse little change in $[Ca]_i$ was visible. In trials where the prepulse was 15 s or less, latency was shortened in all 11 cells tested (Fig. 2 *B*). The effect was smallest in cells with short latencies, and in these cases the prepulse itself always caused Ca release. The decrease in latency was proportional to the length of the prepulse for prepulses up to 15 s long (Fig. 2 *B*). However, a prepulse of 10 μM carbachol lasting 45 s had very little effect on latency (*filled symbol*), much smaller than expected for this agonist exposure expressed in units of (dose × duration) (Fig. 2 *B*, *fitted line*). This indicates that the messenger generated during the long prepulse had decayed during that time.

Determining Single-Cell IP_3 Lifetime from Response Latency

For experiments in which response desensitization was negligible, it was possible to measure latencies to a range of concentrations of carbachol in the same cell. Fig. 3 *A* shows Ca responses to 30, 100, and 300 μM, and 1 mM carbachol. Ca release is slower at lower doses of agonist and the latency is longer. We analyzed the

dependence of latency on agonist dose using a model in which IP_3 accumulates to a threshold to cause Ca release and is degraded with lifetime τ. This model is consistent with the prior observation that gradual photolysis of IP_3 leads to delayed, sharp rises in Ca (Parker and Ivorra, 1992). In this model, higher concentrations of agonist cause greater activation of phospholipase C and faster generation of IP_3. Therefore,

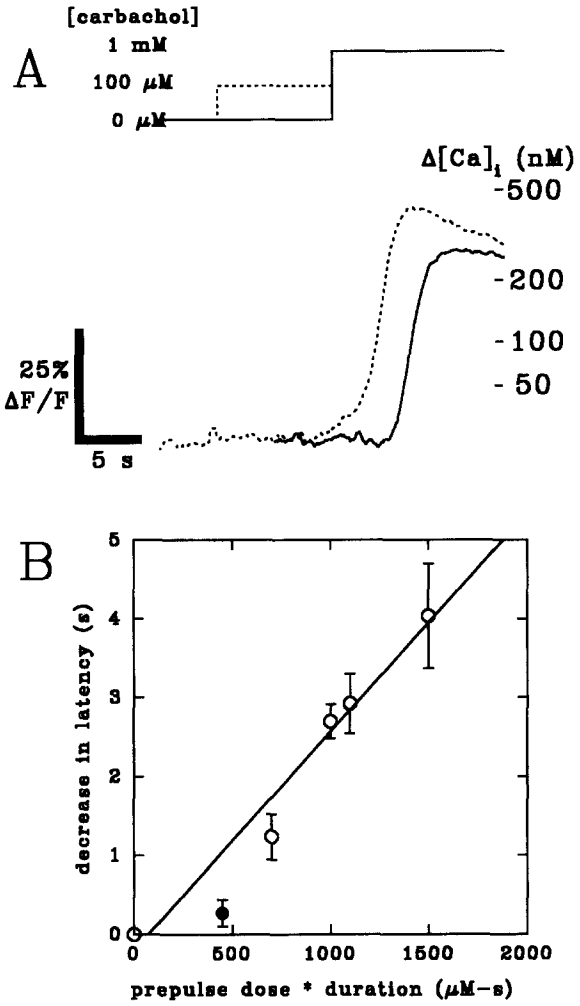

FIGURE 2. Effects of an agonist prepulse on Ca release latency. (*A*) Two recordings from a cell exposed to 1 mM carbachol. For the second (*dashed*) trace the application of 1 mM carbachol was preceded by a prepulse of 100 μM carbachol lasting 10 s. This shortened the latency from 6.6 to 3.6 s. (*B*) Average change in latency for various prepulses. The prepulses are plotted on the x axis as the product (carbachol dose × prepulse duration). The open symbols represent 100 μM carbachol presented for 7, 10, 11, and 15 s. The filled symbol represents 10 μM carbachol for 45 s. Error bars represent SEM. The line is a least-squares fit.

it predicts that latency will decrease with increasing muscarinic receptor occupancy. Furthermore, the relationship between inverse muscarinic receptor occupancy and latency will be an exponential with time constant τ (see Appendix A). A fit to this model for two cells (Fig. 3 *B*) gives IP_3 lifetimes of 5.7 ± 0.5 and 13.4 ± 0.8 s.

In this study the rate constant for IP_3 degradation, $k = 1/\tau$, varied widely over the population of cells and was approximately exponentially distributed (Fig. 3 *C*). Values of k ranged from <0.05 s^{-1} ($\tau > 20$ s) to >0.25 s^{-1} ($\tau < 4$ s). A fit of the

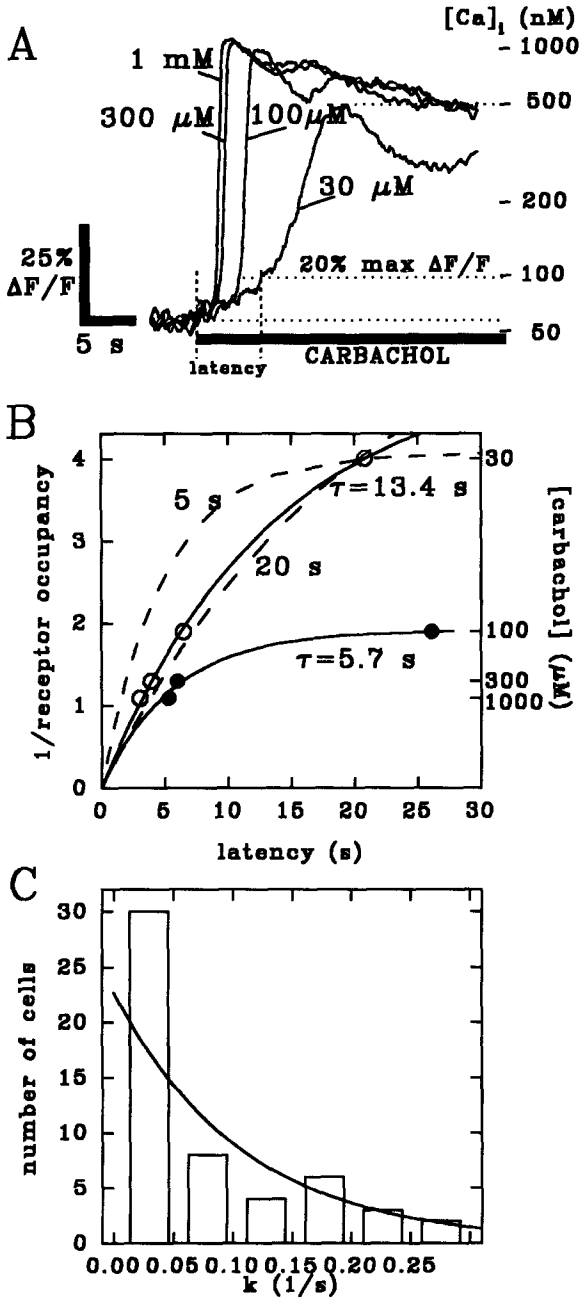

FIGURE 3. Latency analysis to determine single-cell IP_3 degradation rate. (*A*) Ca responses in a single cell to 1 mM, 300 μM, 100 μM, and 30 μM carbachol. (*B*) A fit of latency to inverse muscarinic receptor occupancy in two single cells. Receptor occupancy was calculated according to a single-site model assuming K_D = 100 μM. Open symbols are latencies for the cell of *A*. Data for these two cells were fitted by IP_3 lifetimes (τ) of 5.7 ± 0.5 and 13.4 ± 0.8 s. The fits are indicated by solid lines. For the cell with τ = 13.4 s, the best fits with τ constrained to 5 and 20 s are also shown. (*C*) Distribution of rate constants (k) for 53 single cells, where $k = 1/\tau$. The curve is a least-squares fit of the logarithm of the number of cells against k and follows the equation $22.4\ e^{-9.2k}$.

histogram of values of k to an exponential gave a mean k of $\langle k \rangle = 0.11 \pm 0.03\ s^{-1}$, corresponding to a lifetime of $1/\langle k \rangle = 9.2 \pm 2.2$ s. The arithmetic mean value of k was $0.058 \pm 0.067\ s^{-1}$ (SD, 53 cells in three experiments), and the uncertainty in k was $0.023 \pm 0.027\ s^{-1}$ (SD). In 28% of cells, the latency and inverse muscarinic receptor occupancy were approximately linearly related. Assuming that the longest lifetime detectable by fitting to an exponential is twice the longest latency observed, this corresponds to $\tau > 40$ s.

Measuring IP_3 Lifetime Biochemically

For a heterogeneous population of cells with exponentially distributed k, the overall half life of IP_3 is predicted to be the inverse of the mean of the distribution, $1/\langle k \rangle$ (see Appendix A). We measured the time course of IP_3 degradation in cell populations by direct biochemical determination of IP_3 content before and after exposure to carbachol. The basal level of IP_3 was 10 ± 3 nM ($n = 4$). Cells were stimulated with 1 mM carbachol for 30 s, and after carbachol stimulation, IP_3 content increased 3.5 ± 0.7-fold over basal levels to an estimated 35 ± 10 nM. In parallel experiments, carbachol stimulation was followed by incubation with 10 μM atropine for 10–30 s to block further IP_3 production, and IP_3 was determined at the end of the atropine incubation (Fig. 4). These data show that IP_3 is degraded with a half life of 9 ± 2 s, eventually returning to basal levels.

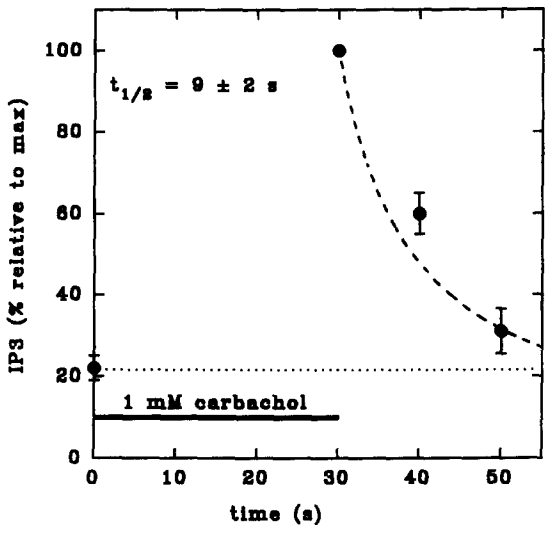

FIGURE 4. Direct biochemical determination of IP_3 content of cells before and after exposure to carbachol. Cells were exposed to 1 mM carbachol for 30 s. The cells were lysed at the end of the carbachol exposure or after replacing carbachol with 10 μM atropine for 10, 20, or 30 s. IP_3 levels were assayed by competitive binding assay as described in Materials and Methods. The IP_3 concentrations in each of four experiments were normalized to basal levels of IP_3. Interpolation to the data give a half life for IP_3 of 9 ± 2 s. The curve is a plot of the expected time course of IP_3 based on the latency analysis (see Appendix A), with a half life of 9.2 s.

Tests of Calcium Feedback Mechanisms: Inhibiting Ca Feedback

Calcium itself might contribute to setting the latency. In this alternative hypothesis, latency is caused by the gradual accumulation of small amounts of Ca that feed back

positively to cause regenerative calcium-induced calcium release (Dupont, Berridge, and Goldbeter, 1990). Ca could also serve to shorten latency by enhancing IP_3 action to cause more Ca release, analogous to the role of depolarization in the initiation of an action potential. If either of these were so, then our latency analysis would not give accurate IP_3 lifetime information. It was therefore important to test for the presence of Ca feedback.

If Ca were playing a positive feedback role in determining the kinetics of release, then it should be possible to decrease the feedback by loading cells with Ca buffers. This treatment would attenuate the rise in free $[Ca]_i$ caused by a small amount of Ca release and therefore prolong latency or rise time.

Ca responses were recorded before and after additional loading with membrane-permeant acetoxymethyl esters of Ca buffers. The addition of BAPTA-series Ca buffers (2–5 μM of AM ester for 30 min) decreased the peak $[Ca]_i$ and slowed release (Fig. 5 *A*). This buffer loading caused the rise time to increase from 2.1 ± 0.4 to 4.6 ± 0.5 s (mean ± SEM, 37 cells in 10 experiments; Fig. 5 *B*). The latency also increased somewhat, from 4.5 ± 0.3 s to 6.3 ± 0.5 s (Fig. 5 *C*). Loading with the nonbuffering compound AM-APDA ("half-BAPTA/AM") (10 μM, 30–50 min) had no effect on latency or rise time, showing that the AM-loading procedure itself had no deleterious effect on the Ca release machinery. The large increase in rise time suggests that Ca exerts significant positive feedback upon Ca release machinery during the rising phase of Ca release. However, it participates to a lesser extent in regulating latency.

If direct calcium-induced calcium release (CICR) contributes to the N1E-115 calcium release signal, then drugs which modulate direct CICR should interfere with calcium release. We applied drugs known to act upon the ryanodine receptor, which is thought to mediate direct CICR (Ashcroft, 1991). The response to 1 mM carbachol was measured first in control conditions, and drugs were applied 8–20 min after carbachol washout. The magnitude of Ca release was then measured during a second application of carbachol 5–10 min later. Ca release was unaffected by the blockers dantrolene (30–100 μM; 111.8 ± 10.4% of control, 29 cells in two experiments) and ryanodine (1 μM; 85.4 ± 15.4% of control, 36 cells in two experiments), or by the channel agonist caffeine (10 mM; 104.5 ± 4.5% of control, 14 cells in one experiment). Ryanodine treatment also had no effect on latency (2.67 ± 0.23 s before, 2.81 ± 0.24 s after; average change 0.14 ± 0.10 s SEM). The latency to Ca release was also unaffected by acute removal of external Ca (Wang and Thompson, 1994).

Response Scaling at Low Agonist Doses

In search of further evidence for the influence of feedback mechanisms on rise time, we compared the dependence of rise time and latency on carbachol dose. Rise times and latencies for the cell of Fig. 3 *A* decreased with higher agonist dose. If the latent and rising phases of release had equal feedback, then they would remain proportional to one another at all agonist doses and it should be possible to match the time courses by scaling the time axis. A transformation of the Ca release kinetics for 300 μM, 100 and 30 μM carbachol is shown in Fig. 6 *A*. In this example, the scaled time course of Ca release at 30 μM carbachol (*dotted trace*) is noticeably more shallow than the other two traces over the entire rising phase. This effect was quantified in the

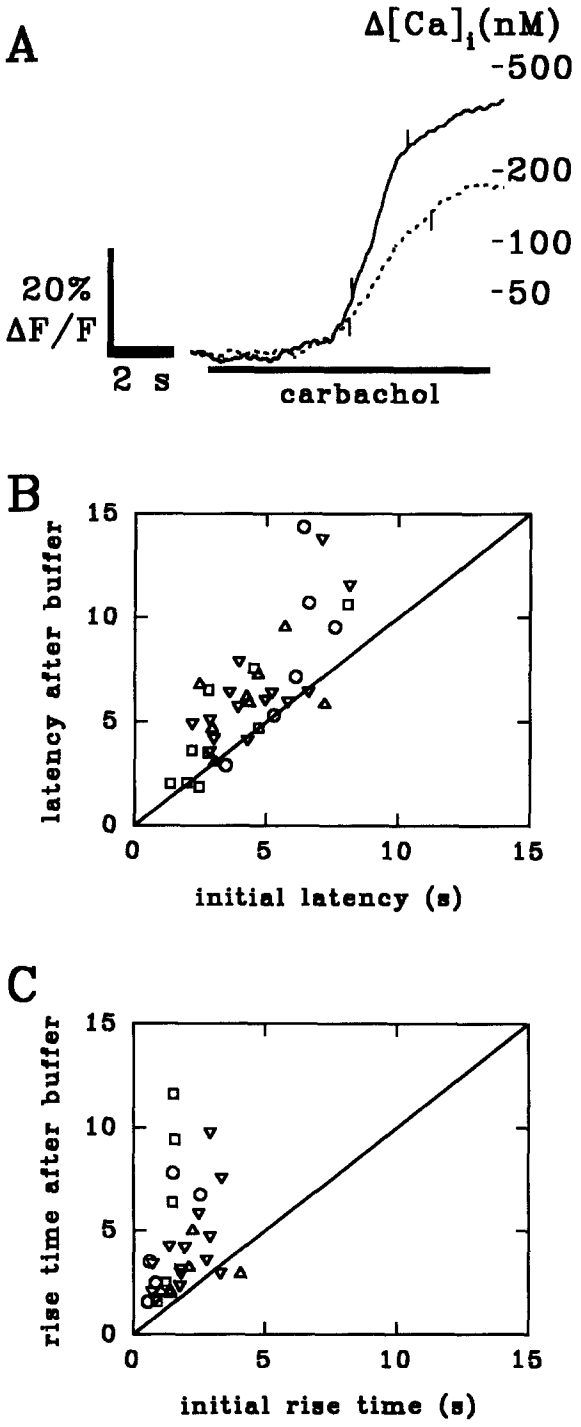

FIGURE 5. Effect of BAPTA-series Ca buffers on Ca release parameters. (*A*) Fura-2/AM effect on a single cell. This cell was challenged once with 1 mM carbachol (*solid line*), and again after a heavy buffer load (*dashed line*). Tick marks indicate latency and the end of the rise time. Ca release was slowed in the rising phase of the response. (*B* and *C*) Scatter plot of (*B*) latency and (*C*) rise time before (abscissa) and after (ordinate) heavy loading with acetoxymethyl esters of various BAPTA-series Ca buffers (37 cells in 10 experiments). Symbols, with (K_D for Ca): □ 5,5′-dimethyl-BAPTA (160 nM); △ BAPTA (590 nM); ▽ 5,5′-dibromo-BAPTA (3.6 μM); and ○ 4,4′-difluoro-BAPTA (4.6 μM). K_D values are in 0 Mg at pH 7.0, 22 ± 1°C (Pethig, Kuhn, Payne, Adler, Chen, and Jaffe, 1989).

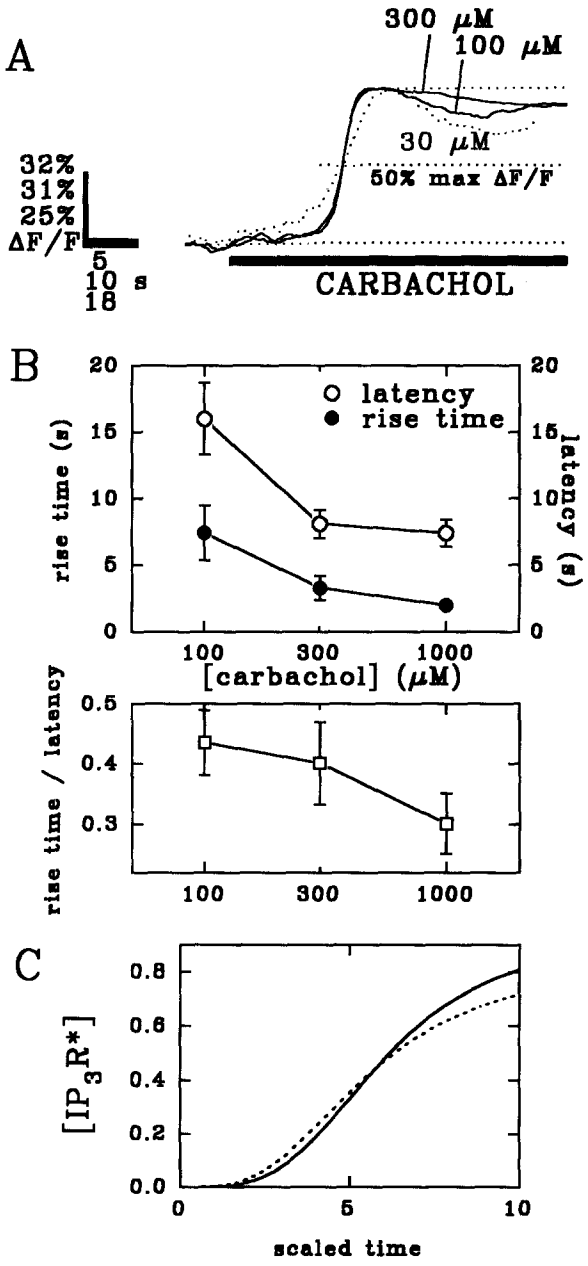

FIGURE 6. Scaling of Ca release kinetics at different agonist doses. (*A*) Ca release for 30, 100, 300, and 1 mM carbachol, scaled to match 50% rise time and ΔF peak. In this example, the time course of Ca release at 30 μM carbachol is noticeably more shallow than the other two traces over the entire rising phase. (*B*) Rise time and latency both decrease with higher carbachol concentration, but their ratio is not constant (*inset*). (*C*) Scaled plot of IP_3 receptor activation, taken from the model of Fig. 9 *C*, showing that IP_3 accumulation might account for the different wave forms at different doses.

single-cell data set as the ratio of rise time to latency, which was 0.44 ± 0.17 (SD) at 100 μM carbachol and 0.30 ± 0.16 at 1 mM carbachol and was higher for the lower agonist dose in 10 of 11 cells (Fig. 6 *B*). This relative shortening of rise time at high agonist doses is consistent with the presence of regenerative Ca feedback in the rising phase of release. However, scaling is exact only if the IP_3 time course is linear, and

the presence of IP_3 degradation predicts that there will be curvature in the IP_3 time course. This curvature is magnified if the action of IP_3 on its receptor is positively cooperative (Fig. 9, *A* and *B*). Since this curvature does not scale (Fig. 6 *C*), it might also be sufficient to explain the lack of scaling of Ca release.

Increasing Feedback by Blocking Ca Pumping Activity

As a means of increasing the amount of feedback caused by calcium, cyclopiazonic acid (CPA) was used to block reuptake of Ca into the ER (Mason, Garcia-Rodriguez, and Grinstein, 1991). Acute exposure to 10 μM CPA for 90 s caused a slow, steady increase in $[Ca]_i$ at a rate of 0.27 ± 0.02% ΔF_{380}/s, or 1.4 ± 0.1 nM $[Ca]_i$/s. The average $[Ca]_i$ was 72 ± 45 nM (SD, 35 cells) before the CPA exposure, 75 ± 51 nM

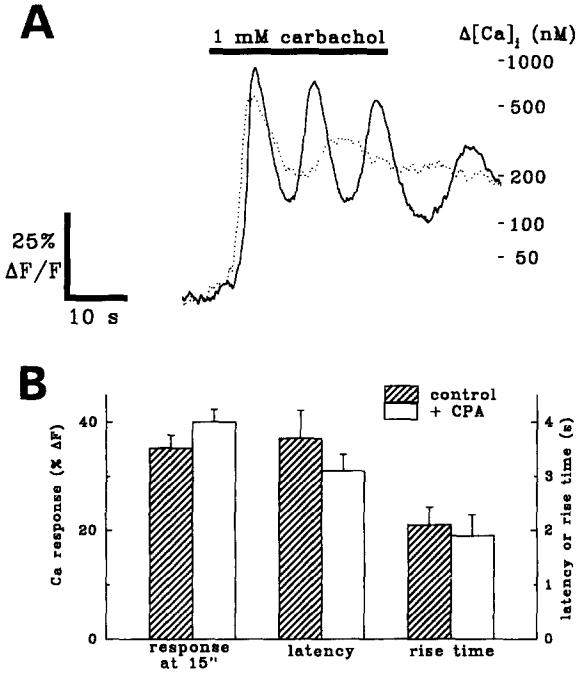

FIGURE 7. Effect of the ER Ca pump blocker cyclopiazonic acid on Ca release. (*A*) Carbachol-evoked Ca responses in a single cell: control (*solid trace*), and after 60 s of treatment with 10 μM CPA (*dotted trace*). The oscillation is attenuated and slowed by CPA. (*B*) The effect of acute (15–60 s) CPA treatment on Ca release (35 cells, 2 experiments), latency (12 cells, 3 experiments), and rise time (12 cells, 3 experiments). Ca release was measured after 15 s of exposure to 1 mM carbachol.

after 15 s, and 103 ± 40 nM after 90 s (17 cells). This rise in $[Ca]_i$ stems at first from leak from the ER, and later from influx through a depletion-activated current. Detailed kinetic studies in these cells using the pump blocker thapsigargin show that the contribution of influx to $[Ca]_i$ is significant after ~30 s (Mathes and Thompson, 1994).

We were interested in the effect of blocking Ca pumping activity acutely, without altering resting $[Ca]_i$ or store content. We therefore measured the effect of CPA treatment on latency at times when pumps were blocked, but before cytoplasmic $[Ca]_i$ had risen significantly. Also, the stores were still full, because acute treatment with CPA did not significantly alter the magnitude of carbachol-evoked Ca release. Cells were challenged once with 1 mM carbachol, and again in a second trial at the end of

a 15–60 s exposure to CPA. Responses were measured after 15 s of exposure to carbachol. The carbachol response was 35.2 ± 2.4% ΔF_{380} ($\Delta[Ca]_i$ = 194 ± 40 nM, SEM) in the control (48 responding cells in three experiments), and 40.0 ± 2.3% ΔF_{380} ($\Delta[Ca]_i$ = 247 ± 50 nM) after CPA treatment (Fig. 7 *B*). Overall, the response size was somewhat increased (mean change 4.8 ± 1.5% ΔF_{380}, 53 ± 11 nM $\Delta[Ca]_i$). However, CPA treatment did appear to attenuate Ca oscillations (Fig. 7 *A*). These observations show that the ability of the ER to mobilize Ca was not compromised by acute CPA treatment, but that Ca oscillations later in the response require ER Ca pump activity.

If the latent period is terminated in part by positive Ca feedback, then blocking ER Ca pumps with CPA might shorten latencies by reducing the rate at which released Ca is cleared from the cytoplasm. We therefore measured the effect of CPA on carbachol-evoked Ca release, and found that neither latency nor rise time was significantly changed by acute CPA treatment (Fig. 7 *B*). The average latency was 3.7 ± 1.7 s (SD) to the first dose of carbachol, and 3.1 ± 1.0 s after CPA exposure (12 cells, three experiments). On average, the change in latency was −0.56 ± 0.39 s (SEM; not significant by *t* test, $P > 0.1$). Rise times were 2.1 ± 1.1 s at first, and 1.9 ± 1.3 s after CPA treatment (average change, −0.22 ± 0.26 s, SEM; not significant, $P > 0.4$).

DISCUSSION

We have measured the lifetime of IP_3 in two ways: physiologically by analysis of latency to Ca release, and by direct biochemical determination. The methods both give an average half life of 9 s, showing that at least one parameter of Ca release in single cells, response latency, can be explained in part by a biochemical parameter, the degradation rate constant of IP_3. This rate varied greatly from cell to cell, suggesting that the ability of individual cells to integrate IP_3-mediated signals is similarly variable.

Latency Stems from Messenger Accumulation

The latent period that follows agonist application can be accounted for by the accumulation of a messenger to a threshold level necessary for the initiation of Ca release. In individual cells, latency becomes shorter with increasing doses of carbachol, indicating that increased muscarinic receptor occupancy leads to a faster accumulation of messenger. Furthermore, exposure to a brief, subthreshold level of carbachol is able to prime a cell in the absence of a visible change in $[Ca]_i$, so that the latency to a dose of agonist becomes shorter. The primary candidate for this accumulating messenger is IP_3.

Contribution of Calcium Feedback to Latency

Calcium-induced calcium release has been proposed as a mechanism for ending latency, either by direct calcium-induced calcium release involving ryanodine receptors (Dupont et al., 1990) or by positive Ca feedback acting upon IP_3 receptors (Keizer and De Young, 1992; Dupont and Goldbeter, 1993). In N1E-115 cells,

calcium release is unaffected by ryanodine receptor modulators, indicating that direct CICR does not contribute to agonist-evoked Ca release. Additional loading with fura-2, however, slowed Ca release during the rising phase, suggesting that Ca feedback participates during this part of the response. The effect on latency was smaller, but may also reflect some degree of Ca feedback before IP_3 levels reach threshold.

Experiments with cyclopiazonic acid, an inhibitor of the ER Ca/ATPase, do not provide evidence that positive Ca feedback plays a role in setting latency. CPA was able to block Ca oscillations, but did not change either latency or rise time. However, because IP_3R and Ca/ATPases are separate molecular entities, blocking pumps would not necessarily increase feedback near an IP_3 receptor, because Ca pumping does not play a significant role in attenuating Ca concentration profiles near channels (Roberts, Jacobs, and Hudspeth, 1991). Calcium waves, on the other hand, are thought to rely on local amplification by calcium diffusion (Jaffe, 1991), but blocking or overexpressing Ca pumps in oocytes does not affect the speed of Ca waves (Camacho and Lechleiter, 1993). That result is consistent with our findings if CPA enhances global Ca accumulations, but the Ca feedback that takes place in a Ca wave occurs between nearby channels.

IP_3 Threshold Mechanism for Response Latency

The steep dose dependence of IP_3 acting to promote Ca release suggests either cooperativity of IP_3 action at its receptor, or local feedback by Ca between IP_3 receptors. When combined with the assumption of gradual IP_3 accumulation to threshold, this phenomenon provides an explanation for the quiescent period preceding Ca release. One specific mechanism could be that positive cooperativity of IP_3 action on its receptor (Meyer et al., 1988) causes the rate of Ca release to increase sigmoidally with a linear increase in IP_3 concentration. In this case, the IP_3 threshold is operationally defined as the point of steepest slope on the dose-response curve of IP_3 action upon its receptor; this occurs when $[IP_3] = K_D$ (Fig. 9 *B*).

Alternately, the key step in generating an IP_3 threshold may be local feedback by Ca from one IP_3 receptor to increase the open probability of other IP_3 receptors. Ca feedback on IP_3 receptors has been observed at micromolar levels of Ca (Iino, 1990; Bezprozvanny, Watras, and Ehrlich, 1991; Finch, Turner, and Goldin, 1991). During the latent period this would only be achieved in the domain immediately surrounding an open IP_3 receptor channel. At low levels of IP_3 (Fig. 8, *top*), IP_3-bound receptors would be farther apart than the size of a domain, and so Ca release from one channel would not be able to reach other channels to cause further channel opening. As IP_3 levels rise, the average distance between bound receptors decreases, and when bound IP_3 receptors are closer to one another than the size of a domain, Ca from one open channel can cause further release from nearby channels (Fig. 8, *bottom*). Threshold for this regenerative effect is reached when the distance between IP_3-bound receptors is smaller than the size of a single-channel Ca domain. The IP_3 threshold is then set by a number of parameters, including the affinity of the receptor for IP_3, its sensitivity to Ca, the mean distance between receptors, and the size of a Ca domain.

Analyzing Latency for IP_3 Lifetime

Either of these two mechanisms leads to a sharp rise in Ca as IP_3 rises past a threshold level. A threshold mechanism of calcium rise was first suggested by Horn and Marty (1988) to explain the time course of muscarinic receptor-coupled potassium current activation in lacrimal gland cells. Our principal modification of the IP_3-accumulation model is the addition of a degradative process for the removal of IP_3. Because the dependence of latency on inverse muscarinic receptor occupancy is curved toward the latency axis, this modification is necessary in order to satisfactorily explain the data. A degradative process has previously been assumed in order to explain latency to Ca release evoked by slow photolysis of caged IP_3 in *Xenopus* oocytes (Parker and Ivorra, 1992).

A consequence of this analysis is that we have observed a large cellular variation in IP_3 degradation rates that is not detectable by biochemical determinations. Indeed, in 28% of the cells we examined, the latency inverse muscarinic receptor occupancy

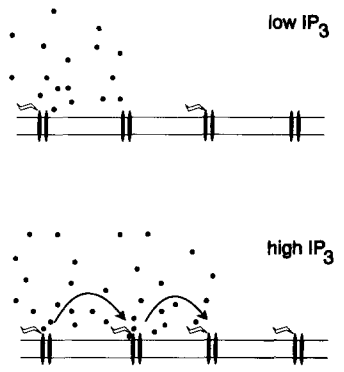

FIGURE 8. A hypothetical regenerative model of latency to Ca release. IP_3 accumulates slowly in cytoplasm. At low IP_3 levels (*top*), IP_3 receptors bound to IP_3 can open with low probability, but nearby receptors are not bound by IP_3, and Ca release is confined to Ca domains near isolated channels. As IP_3 rises to threshold (*bottom*), the distance between bound receptors decreases, until IP_3-bound receptors are spaced more closely than the size of a Ca domain. At this point, Ca release from one channel increases the open probability of nearby IP_3-bound channels, allowing regenerative Ca release.

plot appeared linear, indicating very little IP_3 degradation. Variability in the concentration of IP_3 degradation enzymes would confer different abilities to integrate IP_3 signals in different cells. This is a feature of potential importance in many systems, including dendritic spines (Koch and Zador, 1993). It could also contribute to the expression of delayed rises in Ca, sites of wave initiation, and stereotyped wave patterns of intercellular Ca waves, all of which have been observed in glial cells (Cornell-Bell, Finkbeiner, Cooper, and Smith, 1990).

Errors of IP_3 Lifetime Estimation from the Latency Analysis

This latency analysis is subject to three types of potential error: (*a*) latency does not arise entirely from messenger accumulation; (*b*) the accumulating messenger is not entirely IP_3; and (*c*) the IP_3 threshold may be dependent on agonist dose.

In addition to accumulation of a second messenger, rate-limiting steps before PLC activation may also contribute to the latent period (for a discussion see Marty, Horn, Tan, and Zimmerberg, 1989). These steps include binding of agonist-bound receptor

to G protein, activation of the G_α subunit, and G_α binding to and activation of PLC. All of these steps take place in <1 s (Vuong, Chabre, and Stryer, 1984; Berstein, Blank, Jhon, Exton, Rhee, and Ross, 1992). This matches the observation that the minimum latency to Ca release observed after receptor activation is <1 s (Horn and Marty, 1988; Neher, Marty, Fukuda, Kubo, and Numa, 1988; Marty and Tan, 1989). These steps, therefore, would not be able to generate latencies of the length we have observed.

A minimum latency inherent to the transduction machinery (Fuortes and Hodgkin, 1964) would shift the inverse bound receptor concentration, 1/[B], vs latency curve to the right. We subtracted a 0.5-s minimum latency from the examples of Fig. 3 *B* and found that the fitted IP_3 lifetimes decreased very little, from 5.7 s to 5.1 s, and from 13.4 s to 11.2 s.

Saturation of PLC activation would shift the curve upward at high agonist doses, because PLC activation would be lower than predicted from muscarinic receptor occupancy. This would lead to underestimation of the IP_3 lifetime. However, N1E-115 cells have "spare receptors" in, at most, 5% of cells (Fisher and Snider, 1987; Wang and Thompson, 1994), ruling out major distortions by this effect.

Ca feedback might also accelerate the end of the latent period, and if so, this would give latency values that do not depend solely on IP_3 formation and degradation. We have not found evidence for Ca feedback in determining latency in N1E-115 cells, either by augmenting Ca rises with a Ca pump blocker, or by attenuating Ca rises with heavy buffer loads.

The threshold for Ca release could vary with agonist dose if the IP_3 receptor desensitizes or inactivates during the latent period, since this would lead to an IP_3 threshold that depended on the rate of IP_3 increase. Ca-dependent inactivation of the IP_3 receptor has been observed to take place in <1 s (Finch et al., 1991; Iino and Endo, 1992), but this is too rapid to cause differential effects between a fast and slow rise in IP_3. Use-dependent inactivation of IP_3 receptors has also been observed, with onset and recovery rates in the range of seconds (Parker and Ivorra, 1990). We would not expect to observe this form of IP_3 receptor desensitization during the latent period, a time before significant Ca release has begun.

Biochemical Analysis

The biochemical measurement of IP_3 degradation gave the same value for the half life for IP_3 that was predicted by the latency analysis. This lends support to latency analysis as a means of determining IP_3 lifetime in single cells. Both methods were applied to intact cells under physiological conditions. The latency analysis and the biochemical determination could still conceivably give different results for IP_3 lifetime, since they are based on observations made at low calcium (latency) and at high or falling calcium (biochemical measurement). The IP_3 3-kinase is known to be activated by Ca (Biden and Wollheim, 1986; Takazawa, Lemos, Delvaux, Lejeune, Dumont, and Erneux, 1990). Because biochemical measurement of IP_3 breakdown was made under a condition of cell activation and Ca elevation, the lifetime of IP_3 during latency may be longer than our biochemical measurement. Additional determinations of IP_3 lifetime in cells with Ca release suppressed will resolve this issue.

The IP_3 half life of 9 s is within the range of values reported in other preparations. In experiments that separated IP_3 from inositol (1,3,4) trisphosphate, Irvine et al. (1985) showed that IP_3 produced in response to carbachol was degraded with a half-life of ~1 min. In rat cerebellar microsomes, degradation of IP_3 occurs more rapidly, with a half life of ~5 s (Stauderman, Harris, and Lovenberg, 1988). However, the 3-kinase in rat cerebellum is heterogeneously distributed, with high densities of antibody staining occurring in dendritic spines of Purkinje and basket cells (Yamada, Kakita, Mizuguchi, Rhee, Kim, and Ikuta, 1992), suggesting that the lifetime of IP_3 in these structures is shorter than the biochemical determination. In the extreme case of olfactory cells, IP_3 levels have been observed to rise and fall in 0.1 s or less (Breer et al., 1990).

The variation in lifetime among these cell types may reflect different signaling roles for IP_3. The endocrine function of parotid glands is modulated over minutes, whereas sensory neurons respond to odorants in a fraction of a second. Likewise, a short lifetime of IP_3 would also put spatial and temporal limits on the extent of IP_3 signaling in an extended structure such as a dendritic arbor.

The rise in total IP_3 concentration from 10 nM to 35 nM is consistent with known information on IP_3 receptor properties. N1E-115 cells express Type 3 IP_3 receptors (J. S. Coggan, I. K. Kovacs, and S. H. Thompson, unpublished results), which have a measured affinity for IP_3 of 29 (Yamamoto-Hino, Sugiyama, Hikichi, Mattei, Hasegawa, Sekine, Sakurada, Miyawaki, Furuichi, Hasegawa, and Mikoshiba, 1994) to 151 nM (Maranto, 1994). This is consistent with the idea that stimulation of muscarinic receptors leads to a significant increase in the number of bound IP_3 receptors.

Implications for Calcium Oscillations and Waves

Information on the lifetime of IP_3 is necessary for experimental analysis and quantitative modeling of Ca oscillations. In models of Ca oscillation the lifetime of IP_3 is assumed or inferred from measurements from whole tissue (Meyer and Stryer, 1988; Keizer and De Young, 1992). Our work in N1E-115 cells shows that this parameter can vary over a fivefold range among individual cells even in a clonal cell line.

The relatively long lifetime of IP_3 imposes a requirement that a successful model of Ca release must allow Ca oscillations to occur with, at most, small peak-to-peak changes in IP_3. We observe agonist-evoked calcium oscillations in N1E-115 cells with periods as fast as 3 s (Wang and Thompson, unpublished observations). Assuming $\tau = 10$ s, in a fast Ca oscillator no more than 14% of IP_3 that was present at the peak of the oscillation would be destroyed by the time of the trough. This is an upper limit to the peak-to-peak variation, because it does not consider the additional contribution of continued IP_3 generation. This implies that IP_3 oscillation may not be necessary for generating Ca spikes, and indeed, a constant level of IP_3 receptor stimulation causes Ca oscillations (Wakui, Potter, and Petersen, 1989; Lechleiter and Clapham, 1992; DeLisle and Welsh, 1992). However, if the variations in IP_3 straddle a region of the dose-response activation curve of the IP_3 receptor that is steep because of positive cooperativity, then a small-amplitude IP_3 oscillation might still have functional significance in making a calcium oscillation.

Our experiments show that unlike response latency, the rise time of the Ca signal has a strong Ca feedback component. This is supported by the observation that on a very short time scale, Ca acts locally and positively to cause more Ca release from IP_3-sensitive stores (Finch et al., 1991; Iino and Endo, 1992). Further exploration of this possibility requires the study of events that depend on local feedback. One model for such a study would be the propagation of Ca waves across cells.

APPENDIX A

IP_3 Accumulation Model of Latency

We modeled the accumulation of IP_3 in cytoplasm as a process in which IP_3 is generated by activated PLC (PLC*) in a muscarinic receptor occupancy-dependent manner. The steps leading to IP_3 formation are the association of carbachol with muscarinic receptors, activation of α-subunits of the G protein by agonist-receptor complex, and association of G_α with PLC to form PLC*. All of these steps are rapid. Receptors can associate with and activate G proteins in milliseconds (Vuong et al., 1984). Furthermore, PLCβ1 has been demonstrated to act as a GTPase activating protein (Berstein et al., 1992), so that once activated, PLC molecules are inactivated in < 1 s. This means that in response to a step rise in agonist, [PLC*] jumps to a new equilibrium in 1 s or less (Fig. 9 *A*). Feedback by the other branch of the signaling pathway, via protein kinase C, does not occur in N1E-115 cells (Wang, Mathes, and Thompson, 1993).

If there are no saturating steps in this activation sequence then [PLC*] is proportional to the rate at which it is activated, and therefore proportional to the amount of bound receptor. Saturation in the signaling cascade would appear as a leftward shift in the dose-response curve relative to the receptor binding curve. This does not occur for muscarinic M1 receptors in N1E-115 cells, because the binding K_D for carbachol is 100 ± 5 μM (McKinney and Richelson, 1986) and the carbachol concentration needed for half-maximal activation of Ca release is 96 ± 8 μM (Wang and Thompson, manuscript in preparation).

When IP_3 degradation is considered, the kinetics of IP_3 in a cell are governed by the equation

$$d[IP_3]/dt = k_1[B] - k_2[IP_3], \tag{1}$$

where $[B]$ is the concentration of bound receptor, which for single-site receptor binding to carbachol ($[C]$) satisfies the relation $[B] = [C]/(K_D + [C])$. The principal degradative enzyme, the 3-kinase, has K_m = 0.6–1.5 μM (Irvine, Letcher, Heslop, and Berridge, 1986; Biden and Wollheim, 1986). The affinity of IP_3 for its neuronal receptor is in the nanomolar range (Furuichi, Yoshikawa, Miyawaki, Wada, Maeda, and Mikoshiba, 1989; Yamamoto-Hino et al., 1994; Maranto, 1994), and our measurements likewise give low nanomolar concentrations of IP_3 after agonist presentation. At these concentrations the degradative enzyme is not saturated, and so k_2 is approximately constant during the latent period when IP_3 receptors are not yet activated.

For the initial condition $[IP_3] = 0$ at $t = 0$, the solution of Eq. 1 is $[IP_3] = [B]k_1/k_2(1 - e^{-k_2t})$. Because the dose-response curve of IP_3 action upon its receptor to induce Ca release is steep (Meyer, Holowka, and Stryer, 1988; Parker and Ivorra, 1992), Ca

release will increase sharply as IP_3 builds up to a threshold I_{thr} (Fig. 9 *A* and *B*). The latency L in a single cell should, therefore, fit the expression

$$I_{thr} = [B]k_1/k_2(1 - e^{-k_2L}). \quad (2)$$

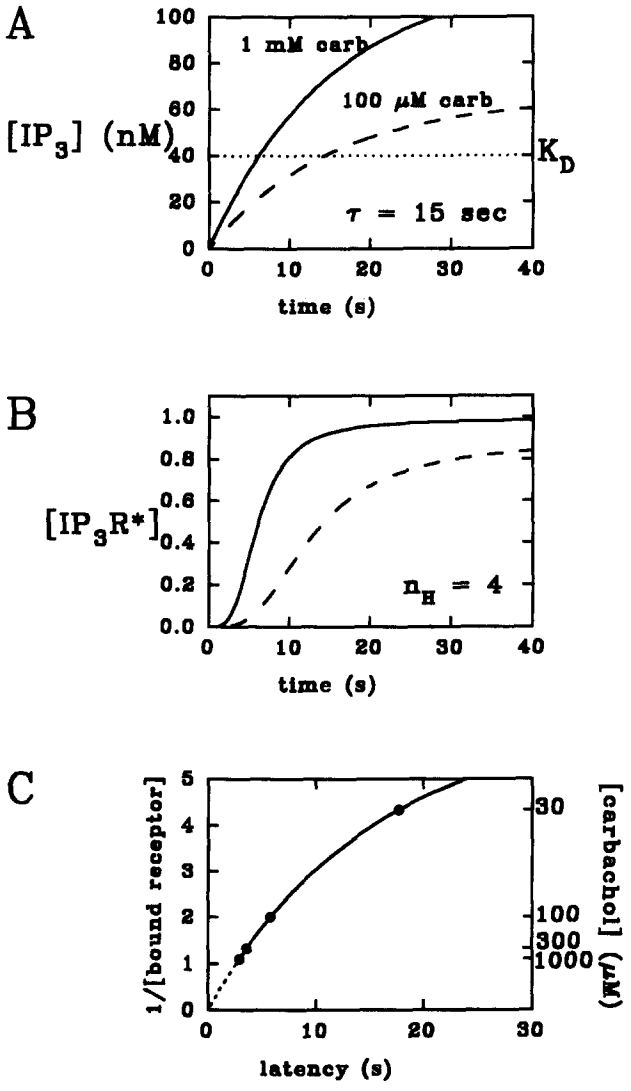

FIGURE 9. Model for Ca response latency in N1E-115 cells. (*A* and *B*) An IP_3-dependent model of latency. IP_3 is generated at a constant rate upon addition of agonist and degraded with time constant τ. As [IP_3] rises past a threshold, Ca release begins sharply, either because of positive cooperativity of IP_3 action upon its receptor (*B*), or regenerative Ca feedback (see Fig. 8). (*C*) Predicted relationship between latency L and inverse muscarinic receptor occupancy 1/[B] in a single cell. The curve is an exponential function with time constant τ (see Appendix A).

This solution allows us to find the lifetime of IP_3 in single cells. Rearrangement of Eq. 2 gives

$$1/[B] = k_1\tau/I_{thr}(1 - e^{-L/\tau}), \quad (3)$$

showing that a plot of $1/[B]$ vs L (Fig. 9 *C*) will take the form of a single exponential with time constant $\tau = 1/k_2$, where τ is the single-cell lifetime of IP_3. A fit of this plot

to a single exponential will therefore give a measure of the rate at which a single cell degrades IP_3. The initial condition $[IP_3] = 0$ was chosen for simplicity of presentation, but the interpretation is the same if some nonzero resting level of IP_3 is assumed. We measured latencies in single cells for a range of agonist doses and fitted these data to Eq. 3 to obtain τ, using a Marquardt nonlinear curve fitting algorithm (Bevington, 1969). We used $K_D = 100$ μM to compute $1/[B]$, assuming single-site binding to the M1 receptor.

This analysis is a biochemical enzyme assay performed on single cells, with inverse latency as the measure of IP_3 production. In the case of no IP_3 degradation ($k_2 = 0$) the relation between inverse muscarinic receptor occupancy and latency is linear and is equivalent to a Lineweaver-Burk double-reciprocal plot, with K_D corresponding to K_m and L corresponding to $1/V$. A model of IP_3 production without degradation has been used to model delays in receptor-evoked responses (Neher et al., 1988; Marty, Horn, Tan, and Zimmerberg, 1989).

The Expected Time Course of IP_3 in Cell Populations

If the degradation of IP_3 follows first-order kinetics, then after a pulse of carbachol, the IP_3 level in single cells will drop exponentially as I_0e^{-kt}, where I_0 is the IP_3 concentration at the end of the carbachol pulse. If the rate constants are exponentially distributed in the population with mean rate constant $\langle k \rangle$, the average time course of IP_3 can be calculated by integrating the single-cell time courses over the population, assuming I_0 is independent of k:

$$[IP_3] = \int (\text{single-cell time course})(\text{probability distribution of rate constants})\, dk$$

$$= \int I_0 e^{-kt} \cdot \frac{1}{\langle k \rangle} e^{-k/\langle k \rangle}\, dk = \frac{I_0}{1 + \langle k \rangle t}.$$

In this time course, $[IP_3]$ falls to half its level at the end of the pulse at $t_{1/2} = 1/\langle k \rangle$.

We thank the staff of the Hopkins Marine Station for excellent support through the course of this work, and M. K. Meffert for advice on IP_3 determinations.

S. Thompson was supported by NIH NS14519. S. Wang was supported by NIH MH10088.

Original version received 2 May 1994 and accepted version received 17 October 1994.

REFERENCES

Allbritton, N. L., T. Meyer, and L. Stryer. 1992. Range of messenger action of calcium ion and inositol 1,4,5-trisphosphate. *Science.* 258:1812–1815.

Ashcroft, F. M. 1991. Ca^{2+} channels and excitation-contraction coupling. *Current Opinion in Cell Biology.* 3:671–675.

Berridge, M. J. 1990. Calcium oscillations. *Journal of Biological Chemistry.* 265:9583–9586.

Berridge, M. J., and R. F. Irvine. 1989. Inositol phosphates and cell signalling. *Nature.* 341:197–205.

Berstein, G., J. L. Blank, D.-Y. Jhon, J. H. Exton, S. G. Rhee, and E. M. Ross. 1992. Phospholipase C-β1 is a GTPase-activating protein for $G_{q/11}$, its physiologic regulator. *Cell.* 70:411–418.

Bevington, P. R. 1969. Data Reduction and Error Analysis for the Physical Sciences. McGraw-Hill, NY. 336 pp.

Bezprozvanny, I., J. Watras, and B. E. Ehrlich. 1991. Bell-shaped calcium-response curves of Ins(1,4,5)P3- and calcium-gated channels from endoplasmic reticulum of cerebellum. *Nature.* 351:751–754.

Biden, T. J., and C. B. Wollheim. 1986. Ca^{2+} regulates the inositol tris/tetrakisphosphate pathway in intact and broken preparations of insulin-secreting RINm5F cells. *Journal of Biological Chemistry.* 261:11931–11934.

Breer, H., I. Boekhoff, and E. Tarelius. 1990. Rapid kinetics of second messenger formation in olfactory transduction. *Nature.* 345:65–68.

Camacho, P., and J. D. Lechleiter. 1993. Increased frequency of calcium waves in *Xenopus laevis* oocytes that express a calcium-ATPase. *Science.* 260:226–229.

Cornell-Bell, A. H., S. M. Finkbeiner, M. S. Cooper, and S. J. Smith. 1990. Glutamate induces calcium waves in cultured astrocytes: long-range glial signaling. *Science.* 247:470–473.

DeLisle, S., and M. J. Welsh. 1992. Inositol trisphosphate is required for the propagation of calcium waves in *Xenopus* oocytes. *Journal of Biological Chemistry.* 267:7963–7966.

Dupont, G., M. J. Berridge, and A. Goldbeter. 1990. Latency correlates with period in a model for signal-induced Ca^{2+} oscillations based on Ca^{2+}-induced Ca^{2+} release. *Cell Regulation.* 1:853–861.

Dupont, G., and A. Goldbeter. 1993. One-pool model for Ca^{2+} oscillations involving Ca^{2+} and inositol 1,4,5-trisphosphate as co-agonists for Ca^{2+} release. *Cell Calcium.* 14:311–322.

Finch, E. A., T. J. Turner, and S. M. Goldin. 1991. Calcium as a coagonist of inositol 1,4,5-trisphosphate-induced calcium release. *Science.* 252:443–446.

Fisher, S. K., and R. M. Snider. 1987. Differential receptor occupancy requirements for muscarinic cholinergic stimulation of inositol lipid hydrolysis in brain and in neuroblastomas. *Molecular Pharmacology.* 32:81–90.

Fuortes, M. G. F., and A. L. Hodgkin. 1964. Changes in the time scale and sensitivity in the ommatidia of *Limulus*. *Journal of Physiology.* 172:239–263.

Furuichi, T., S. Yoshikawa, A. Miyawaki, K. Wada, N. Maeda, and K. Mikoshiba. 1989. Primary structure and functional expression of the inositol 1,4,5-trisphosphate-binding protein P_{400}. *Nature.* 342:32–38.

Grynkiewicz, G., M. Poenie, and R. Y. Tsien. 1985. A new generation of calcium indicators with greatly improved fluorescent properties. *Journal of Biological Chemistry.* 260:3440–3450.

Horn, R., and A. Marty. 1988. Muscarinic activation of ionic currents measured by a new whole-cell recording method. *Journal of General Physiology.* 92:145–159.

Iino, M. 1990. Biphasic Ca^{2+} dependence of inositol 1,4,5-trisphosphate-induced Ca release in smooth muscle cells of the guinea pig taenia caeci. *Journal of General Physiology.* 95:1103–1122.

Iino, M., and M. Endo. 1992. Calcium-dependent immediate feedback control of inositol 1,4,5-trisphosphate-induced Ca^{2+} release. *Nature.* 360:76–78.

Irvine, R. F., E. E. Änggård, A. J. Letcher, and C. P. Downes. 1985. Metabolism of inositol 1,4,5-trisphosphate and inositol 1,3,4-trisphosphate in rat parotid glands. *Biochemical Journal.* 229:505–511.

Irvine, R. F., A. J. Letcher, J. P. Heslop, and M. J. Berridge. 1986. The inositol tris/tetrakisphosphate pathway-demonstration of Ins(1,4,5)P_3 3-kinase activity in animal tissues. *Nature.* 320:631–634.

Jaffe, L. F. 1991. The path of calcium in cytosolic calcium oscillations: a unifying hypothesis. *Proceedings of the National Academy of Sciences, USA.* 88:9883–9887.

Kao, J. P. Y., A. T. Harootunian, and R. Y. Tsien. 1989. Photochemically generated cytosolic calcium pulses and their detection by fluo-3. *Journal of Biological Chemistry.* 264:8179–8184.

Keizer, J., and G. W. De Young. 1992. Two roles for Ca^{2+} in agonist stimulated Ca^{2+} oscillations. *Biophysical Journal.* 61:649–660.

Kimhi, Y., C. Palfrey, I. Spector, Y. Barak, and U. Z. Littauer. 1976. Maturation of neuroblastoma cells in the presence of dimethylsulfoxide. *Proceedings of the National Academy of Sciences, USA.* 73:462–466.

Kimura, Y., Y. Oda, T. Deguchi, and H. Higashida. 1992. Enhanced acetylcholine secretion in neuroblastoma × glioma hybrid NG108-15 cells transfected with rat choline acetyltransferase cDNA. *FEBS Letters.* 314:409–412.

Koch, C., and A. Zador. 1993. The function of dendritic spines: devices subserving biochemical rather than electrical compartmentalization. *Journal of Neuroscience.* 13:413–422.

Lechleiter, J. D., and D. E. Clapham. 1992. Molecular mechanisms of intracellular calcium excitability in *X. laevis* oocytes. *Cell.* 69:283–294.

Maranto, A. R. 1994. Primary structure, ligand binding, and localization of the human Type 3 inositol 1,4,5-trisphosphate receptor expressed in intestinal epithelium. *Journal of Biological Chemistry.* 269:1222–1230.

Marty, A., R. Horn, Y. P. Tan, and J. Zimmerberg. 1989. Delay of the Ca mobilization response to muscarinic stimulation. *In* Secretion and Its Control. G. S. Oxford and C. M. Armstrong, editors. Rockefeller University Press, NY. 98–110.

Marty, A., and Y. P. Tan. 1989. The initiation of calcium release following muscarinic stimulation in rat lacrimal glands. *Journal of Physiology.* 419:655–687.

Mason, M. J., C. Garcia-Rodriguez, and S. Grinstein. 1991. Coupling between intracellular Ca^{2+} stores and the Ca^{2+} permeability of the plasma membrane: comparison of the effects of thapsigargin, 2-5-di-(tert-butyl)-1,4-hydroquinone, and cyclopiazonic acid in rat thymic lymphocytes. *Journal of Biological Chemistry.* 266:20856–20862.

Mathes, C., and S. H. Thompson. 1994. Calcium current activated by muscarinic receptors and thapsigargin in neuronal cells. *Journal of General Physiology.* 104:107–122.

Mathes, C., S. S.-H. Wang, H. M. Vargas, and S. H. Thompson. 1992. Intracellular calcium release in N1E-115 cells is mediated by the M1 muscarinic receptor subtype and is antagonized by McN-A-343. *Brain Research.* 585:307–310.

McKinney, M., and E. Richelson. 1984. The coupling of the neuronal muscarinic receptor to responses. *Annual Reviews in Pharmacology and Toxicology.* 24:121–146.

McKinney, M., and E. Richelson. 1986. Muscarinic responses and binding in a murine neuroblastoma clone (N1E-115): cyclic GMP formation is mediated by a low affinity agonist-receptor conformation and cyclic AMP reduction is mediated by a high affinity agonist-receptor conformation. *Molecular Pharmacology.* 30:207–211.

Meyer, T., D. Holowka, and L. Stryer. 1988. Highly cooperative opening of calcium channels by inositol 1,4,5-trisphosphate. *Science.* 240:653–656.

Meyer, T., and L. Stryer. 1988. Molecular model for receptor-stimulated calcium spiking. *Proceedings of the National Academy of Sciences, USA.* 85:5051–5055.

Miledi, R., and I. Parker. 1989. Latencies of membrane currents evoked in *Xenopus* oocytes by receptor activation, inositol trisphosphate and calcium. *Journal of Physiology.* 415:189–210.

Missiaen, L., H. de Smedt, G. Droogmans, and R. Casteels. 1992. Ca^{2+} release induced by inositol 1,4,5-trisphosphate is a steady-state phenomenon controlled by lunimal Ca^{2+} in permeabilized cells. *Nature.* 357:599–602.

Neher, E., and G. J. Augustine. 1992. Calcium gradients and buffers in bovine chromaffin cells. *Journal of Physiology.* 450:273–301.

Neher, E., A. Marty, K. Fukuda, T. Kubo, and S. Numa. 1988. Intracellular calcium release mediated by two muscarinic receptor subtypes. *FEBS Letters.* 240:88–94.

Oldershaw, K. A., A. Richardson, and C. W. Taylor. 1992. Prolonged exposure to inositol 1,4,5-trisphosphate does not cause intrinsic desensitization of the intracellular Ca^{2+}-mobilizing receptor. *Journal of Biological Chemistry.* 267:16312–16316.

Palmer, S., K. T. Hughes, D. Y. Lee, and M. J. O. Wakelam. 1989. Development of a novel, Ins(1,4,5)P_3-specific binding assay. Its use to determine the intracellular concentration of Ins(1,4,5)P_3 in unstimulated and vasopressin-stimulated rat hepatocytes. *Cellular Signalling.* 1:147–156.

Parker, I., and I. Ivorra. 1990. Inhibition by Ca^{2+} of inositol trisphosphate-mediated Ca^{2+} liberation: a possible mechanism for oscillatory release of Ca^{2+}. *Proceedings of the National Academy of Sciences, USA.* 87:260–264.

Parker, I., and I. Ivorra. 1992. Characteristics of membrane currents evoked by photoreleased inositol trisphosphate in *Xenopus* oocytes. *American Journal of Physiology.* 263:C154–165.

Pethig, R., M. Kuhn, R. Payne, E. Adler, T.-H. Chen, and L. F. Jaffe. 1989. On the dissociation constants of BAPTA-type calcium buffers. *Cell Calcium.* 10:491–498.

Rana, R. S., and L. E. Hokin. 1990. Role of phosphoinositides in transmembrane signaling. *Physiological Reviews.* 70:115–164.

Rhee, S. G., P.-G. Suh, S.-H. Ryu, and S. Y. Lee. 1989. Studies of inositol phospholipid-specific phospholipase C. *Science.* 244:546–550.

Roberts, W. M., R. A. Jacobs, and A. J. Hudspeth. 1991. The hair cell as a presynaptic terminal. *Annals of the New York Academy of Sciences.* 635:221–233.

Stauderman, K. A., G. D. Harris, and W. Lovenberg. 1988. Characterization of inositol 1,4,5-stimulated calcium release from rat cerebellar microsomal fractions. *Biochemical Journal.* 255:677–683.

Surichamorn, W., C. Forray, and E. E. El-Fakahany. 1990. Role of intracellular Ca^{2+} mobilization in muscarinic and histamine receptor-mediated activation of guanylate cyclase in N1E-115 neuroblastoma cells: assessment of the arachidonic acid release hypothesis. *Molecular Pharmacology.* 37:860–869.

Takazawa, K., M. Lemos, A. Delvaux, C. Lejeune, J. E. Dumont, and C. Erneux. 1990. Rat brain inositol 1,4,5-phosphate 3-kinase: Ca^{2+}-sensitivity, purification and antibody production. *Biochemical Journal.* 268:213–217.

Vuong, T. M., M. Chabre, and L. Stryer. 1984. Millisecond activation transducin in the cyclic nucleotide cascade of vision. *Nature.* 311:659–661.

Wakui, M., B. V. L. Potter, and O. H. Petersen. 1989. Pulsatile intracellular calcium release does not depend on fluctuations in inositol trisphosphate concentration. *Nature.* 339:317–320.

Wang, S. S.-H., C. Mathes, and S. H. Thompson. 1993. Membrane toxicity of the protein kinase C inhibitor calphostin A by a free-radical mechanism. *Neuroscience Letters.* 157:25–28.

Wang, S. S.-H., and S. H. Thompson. 1994. Measurement of changes in muscarinic and histaminergic receptor density in single neuroblastoma cells using calcium release desensitization. *Cell Calcium.* 15:483–496.

Winfree, A. T. 1987. When time breaks down: the three-dimensional dynamics of electrochemical waves and cardiac arrythmias. Princeton University Press, NJ. 340 pp.

Yamada, M., A. Kakita, M. Mizuguchi, S. G. Rhee, S. U. Kim, and F. Ikuta. 1992. Ultrastructural localization of inositol 1,4,5-trisphosphate 3-kinase in rat cerebellar cortex. *Brain Research.* 578:41–48.

Yamamoto-Hino, M., T. Sugiyama, K. Hikichi, M. G. Mattei, K. Hasegawa, S. Sekine, K. Sakurada, A. Miyawaki, T. Furuichi, M. Hasegawa, and K. Mikoshiba. 1993. Cloning and characterization of human Type 2 and Type 3 inositol 1,4,5-trisphosphate receptors. *Receptors and Channels.* 2:9–22.